RESEARCH PAPER

Embankment Dams Overtopping Breach: A Numerical Investigation of Hydraulic Results

Mahdi Ebrahimi[1] · Mirali Mohammadi[1] · Sayed Mohammad Hadi Meshkati[2] · Farhad Imanshoar[3]

Abstract

The overtopping breach is the most probable reason of embankment dam failures. Hence, the investigation of the mentioned phenomenon is one of the vital hydraulic issues. This research paper tries to utilize three numerical models, i.e., BREACH, HEC-RAS, and FLOW-3D for modeling the hydraulic outcomes of overtopping breach phenomenon. Furthermore, the outputs have been compared with experimental model results given by authors. The BREACH model presents a desired prediction for the peak flow. The HEC-RAS model has a more realistic performance in terms of the peak flow prediction, its occurrence time (5-s difference with observed status), and maximum flow depth. The variations diagram in the reservoir water level during the breach process has a descending trend. Whereas it initially ascended; and then, it experienced a descending trend in the observed status. The FLOW-3D model computes the flow depth, flow velocity, and Froude number due to the physical model breach. Moreover, it revealed a peak flow damping equals to 5% and 5-s difference in the peak flow occurrence time at 4-m distance from the physical model downstream. In addition, the current research work demonstrates the mentioned numerical models and provides a possible comprehensive perspective for a dam breach scope. They also help to achieve the various hydraulic parameters computations. Besides, they may calculate unmeasured parameters using the experimental data.

Keywords Dam breach · Physical model · Numerical modeling · BREACH · HEC-RAS · FLOW-3D

1 Introduction

The study of embankment dams overtopping failure is a remarkable subject. This is because the overtopping phenomenon is the most common reason of the embankment dam's failure (Committee on dam safety 2019). Meanwhile, it is affected by several factors, such as dam and reservoir geometric characteristics, dam geotechnical properties, and traits of the flood entering reservoir. Further, it is important in terms of management of life, financial, and environmental consequences. Overtopping refers to the passage of water over the dam crest, which causes erosion and eventual destruction of the dam body. This phenomenon mainly occurs for reasons such as the lack of a suitable spillway to release the flood flow; reduced reservoir storage capacity because of sediment accumulation; and dam settlement (Association of state dam safety officials 2023). The most important objectives in the numerical study of embankment dam failure are to achieve the failure geometry, the flow hydrograph, and hydraulic parameters (flow depth, flow velocity, and Froude number). Because the experimental modeling includes several issues, the mentioned phenomenon is often analyzed by numerical models. Additionally, it is not possible to achieve all of breach hydraulic parameters through experimental setup. Because of damping in flow direction, estimation of breach flow routing using the FLOW-3D model will be important. Moreover, FLOW-3D model can be useful to compute flow hydraulic parameters.

✉ Mirali Mohammadi
    m.mohammadi@urmia.ac.ir

    Mahdi Ebrahimi
    ma.ebrahimi@urmia.ac.ir

    Sayed Mohammad Hadi Meshkati
    h_meshkati@yahoo.com

    Farhad Imanshoar
    Imanshoar@gmail.com

1   Department of Civil Engineering (Water & Hydraulic Structures), Faculty of Engineering, Urmia University, P O Box 165, Urmia 57561-51818, Iran

2   Department of Hydraulics and Hydro-Environmental Engineering, Water Research Institute, Tehran, Iran

3   Iranian Water Resources Management Company, Tehran, Iran

A breach geometry looks like a trapezoidal shape, and its most important parameters are observed in Fig. 1 (Brunner 2016a, b). In Fig. 1, h_b = breach section height; B_t = breach section upper width; W_b = breach section lower width; B_{ave} = breach section average width; V = breach section vertical slope; H = breach section horizontal slope; and h_w = overtopping water elevation. There are different stages to analyze the flow hydrograph. An important goal of its measurement is always to determine the peak flow discharge and its occurrence time (Morris et al. 2009).

Several numerical studies have been conducted to determine the overtopping breach results of embankment dams. Wang and Bowles (2006) proposed a 3D model for dam breach. They validated it using IMPACT project data. Morris et al. (2009) explained the modeling of the dam breach initiation and development stages in a FLOOD site project report. In their research, they utilized the numerical modeling outputs based upon laboratory results. Xu & Zhang (2009) developed a nonlinear regression model to predict the embankment dams breach parameters. It was found that the erodibility of the dam was the most influential factor affecting the breach parameters. Pierce et al. (2010) performed a statistical analysis utilizing the linear, nonlinear, and multi-regression models. Wu et al. (2012) developed a 2D model for unsteady flow simulation and non-cohesive sediment transport due to overtopping breach.

Hooshyaripor et al. (2014) analyzed the peak discharge of embankment dams. The results of analysis showed that the ANN technique was better than statistical relationships to predict the peak outflow. Further, the dam height had a greater effect on the peak outflow in comparison with the reservoir water volume. Hakimzadeh et al. (2014) utilized the genetic programming technique to propose a formula for homogeneous models' peak discharge. Its outcomes had a desirable agreement with observational results. Froehlich (2016) presented two nonlinear mathematical models to predict the maximum discharge based on embankment dams breach outflow events. The mentioned models presented more accurate predictions. Azimi and Shabanlou

(2016) studied the changing of the flow free surface and the turbulence of the flow field in triangular channels with side weir. They numerically simulated using volume of fluid scheme and RNG k–ε turbulence model. Azimi et al. (2017) simulated the 3D pattern of hydraulic jumps in U-shaped channels using the FLOW-3D software. According to the numerical modeling results, the standard k–ε turbulence model estimates the flow characteristics with more accuracy. Azimi and Shabanlou (2018) simulated the pattern and the field of the passing flow through circular channels with the side weir in supercritical flow conditions using the FLOW-3D model. A worthy agreement obtained between numerical simulation results and the experimental data. Irmakunal (2019) combined the ArcGIS and HEC-RAS models to study the Berdan dam breach. He determined the high-risk regions at flood plain. Kumar Gupta et al. (2020) utilizing the HEC-RAS model obtained Jawai dam breach parameters. Also, performing the Arc-GIS and HEC-RAS models achieved the submerged areas map. Mo et al. (2023) introduced a new quantitative method for flood risk assessment of Chengbi river dam. Three schemes were proposed for flood simulation by HEC-RAS 2D. The results showed that the greater degree of dam break will cause the greater the inundation depth, maximum flow velocity, and inundation duration. Also, high-risk areas decrease with decreased dam break degree.

As it is clear from the mentioned background; there is a huge gap about predicting of physical models' breach flow properties. Besides, there are few research paying attention to software modeling outcomes and comparing them with experimental results. The present research has attempted to use the capabilities of the BREACH, HEC-RAS, and FLOW-3D models to approximate the breach hydraulic results of the constructed physical model. Furthermore, the obtained outcomes have been compared with experimental results as well as possible. Moreover, the numerical research will make an appropriate prediction on unmeasured hydraulic parameters.

2 Materials and Methods

2.1 Experimental Setup

Physical modeling was performed at the hydraulics laboratory of the Iranian Water Research Institute (IWRI). To achieve the research objectives, a cement channel was constructed measuring 1 m in width and with a slope of 2 in thousand. Before starting the experiments, the sand samples were examined by the soil mechanics laboratory. The optimum moisture content was determined to be 9.2% (ASTM D422-63 2002). The physical model was made in six layers (five layers with a thickness of 5 cm and one layer with
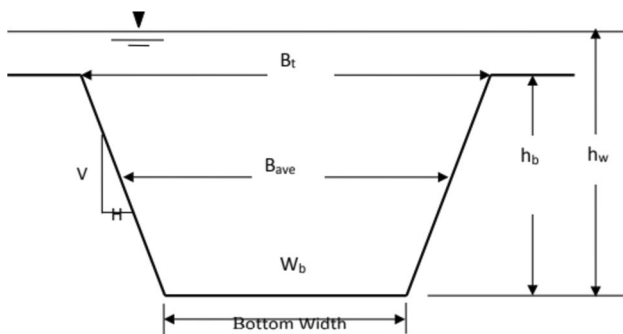

Fig. 1 A schematic dam breach geometry

a thickness of 2 cm). The compaction operation of shell material $(d_{50} = 0.5mm)$ was done by falling flat hammers at optimal humidity percentage and continued to the point where it was no longer possible to vary the volume (ASTM D1557 2007). The physical model was constructed based upon the design principles mentioned in reliable sources (USBR 1987; USACE 2004; Engomoen et al. 2014). Table 1 reports the shell specifications. Six digital cameras placed at appropriate locations to record the breach geometry, the downstream flow hydrograph, and flow levels (Fig. 2). To measure the flow hydrograph, a 90° V-notch weir was utilized at 5.5 m away from the physical model toe. Equation 1 was used to calculate the flow hydrograph (in m³/s) through the 90° V-notch weir (Novak et al. 2017)

Table 1 Shell properties

Height (cm)	Top width (cm)	Bottom width (cm)	Upslope (V:H)	Downslope (V:H)	Weight (kg)	Compaction percent
27	5	159	1:3	1:2.7	296	69
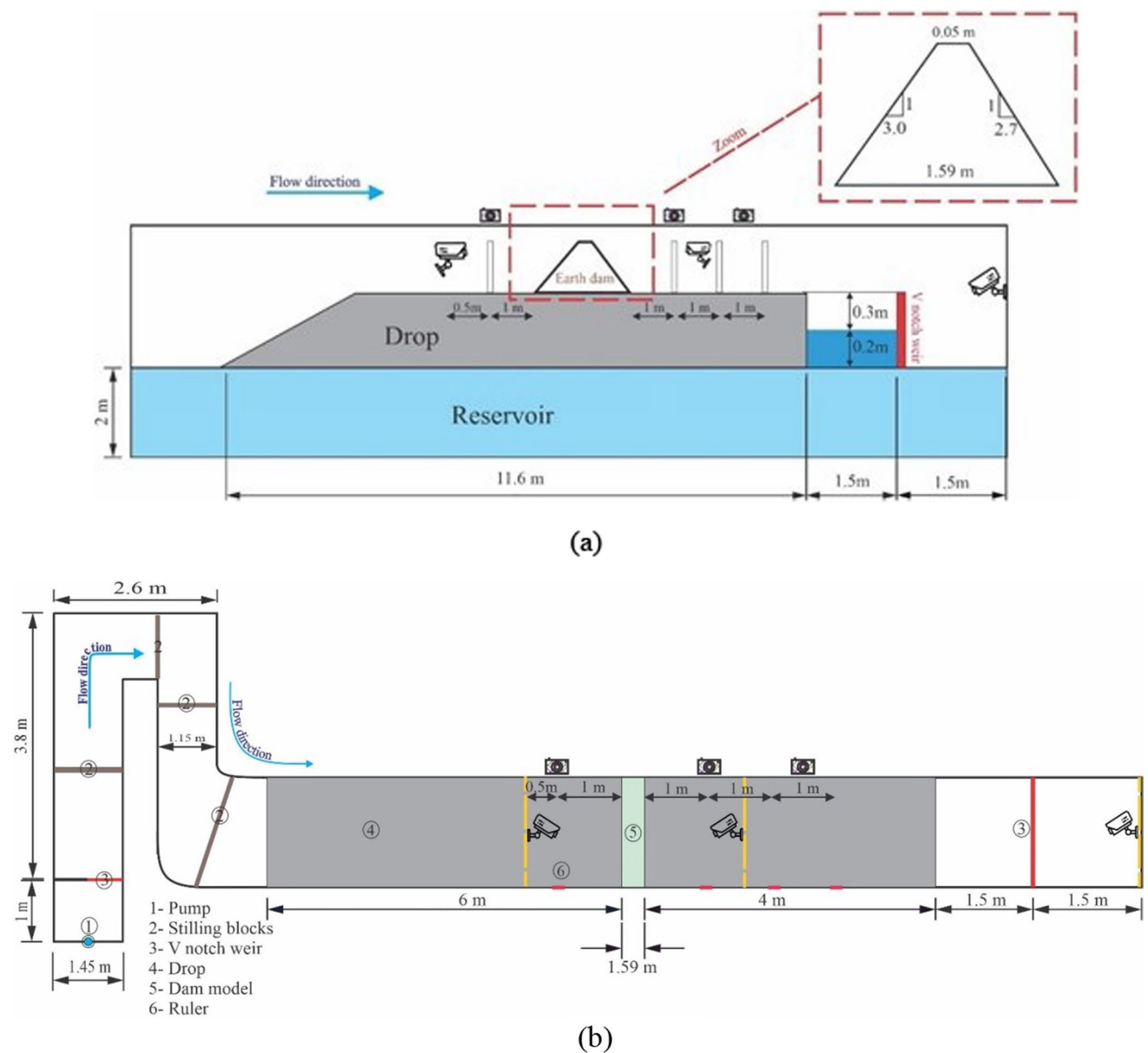
Fig. 2 Experimental setup: **a** side view and **b** plan view

$$Q = \frac{8}{15}\sqrt{2g}C_{d}\tan\left(\frac{\theta}{2}\right)H^{2.5} \tag{1}$$

In the equation above, C_d = discharge coefficient; which is a function of the V-notch angle (θ); and H = water level height on the V-notch (in meters). Chanson and Wang (2013) calibrated a 90° V-notch weir for an unsteady rapidly varied flow; and the results yielded to a discharge coefficient C_d = 0.58. Before initiating the test, a rectangular groove measuring 10 cm in length and 2.5 cm in depth was dug in the crest middle to guide the breach process. The lake volume at breach initiation was 4.3 m^3. The test was repeated to ensure the results. After the completion of the test, the recorded video was saved on the laboratory computer. Accordingly, Plot Digitizer software acquired the breach geometry and flow hydrograph data after accurate calibration procedure. Figure 2 presents a schematic picture for the experimental setup.

2.2 Governing Equations

The breach flow is an unsteady and rapidly varied flow. Its related equation in simplified form is the Saint–Venant equation (Eq. 2); which can be solved by the implicit finite difference method (Novak et al. 2017).

$$S_{f} = S_{0} - \frac{\partial y}{\partial x} - \frac{V}{g}\frac{\partial V}{\partial x} - \frac{1}{g}\frac{\partial V}{\partial t} = \frac{n^{2}V^{2}}{R^{\frac{4}{3}}} \tag{2}$$

In this equation, V = flow velocity; g = acceleration due to gravity; n = Manning roughness coefficient; R = hydraulic radius; S_f = friction slope; and S_0 = channel bed slope. The majority of sediment transport governing equations are written for uniform flow and mild bed slopes conditions. Therefore, using those equations for the breach flow will result many errors. Meyer–Peter & Müller (1948) equation modified by Smart (1984); where it is the most common sediment transport equation. Equation 3 utilized for bed slopes less than 20% (Saberi 2016).

$$q_{b}=4\left(\frac{d_{90}}{d_{30}}\right)^{0.2}\left(\frac{V}{(ghS_{0})^{0.5}}\right)S_{0}^{0.6}\theta^{0.5}(\theta - \theta_{c})[(S_{rel} - 1)gd^{3}]^{0.5} \tag{3}$$

In the above equation, $\theta - \theta_c$ = difference between Shields and critical Shields parameters; S_{rel} = relative density; d = average sediment size diameter (in m); S_0 = bed slope; and q_b = sediment discharge per unit width (in m^2/s). The FLOW-3D model solves the mass conservation and Navier–Stokes equations using the finite volume method to determine the velocity and pressure squares (Eqs. 4–7).

$$V_{F}\frac{\partial \rho}{\partial t} + \frac{\partial(\rho u A_{x})}{\partial x} + \frac{\partial(\rho v A_{y})}{\partial y} + \frac{\partial(\rho w A_{z})}{\partial z} = R_{SOR} + R_{DIF} \tag{4}$$

$$\frac{\partial u}{\partial t} + \frac{1}{V_{F}}\left(uA_{x}\frac{\partial u}{\partial x} + vA_{y}\frac{\partial u}{\partial y} + wA_{z}\frac{\partial u}{\partial z}\right) = -\frac{1}{\rho}\frac{\partial P}{\partial x} + G_{x} + f_{x} \tag{5}$$

$$\frac{\partial v}{\partial t} + \frac{1}{V_{F}}\left(uA_{x}\frac{\partial v}{\partial x} + vA_{y}\frac{\partial v}{\partial y} + wA_{z}\frac{\partial v}{\partial z}\right) = -\frac{1}{\rho}\frac{\partial P}{\partial y} + G_{y} + f_{y} \tag{6}$$

$$\frac{\partial w}{\partial t} + \frac{1}{V_{F}}\left(uA_{x}\frac{\partial w}{\partial x} + vA_{y}\frac{\partial w}{\partial y} + wA_{z}\frac{\partial w}{\partial z}\right) = -\frac{1}{\rho}\frac{\partial P}{\partial z} + G_{Z} + f_{Z} \tag{7}$$

In equations above, (u, v, w) = velocity vector; (A_x, A_y, A_z) = area fraction vector; (G_x, G_y, G_z) = mass acceleration vector; (f_x, f_y, f_z) = viscosity acceleration vector; R_{SOR} = mass source; R_{DIF} = turbulence diffusion; and V_F = volume fraction. The complete explanation of the finite volume method is available in valid books (Versteeg and Malalasekera 2007).

2.3 BREACH Numerical Model

The physical-based model has been designed according to the hydraulic principles. The BREACH model considers erosion process in which the breach section is assumed to be either rectangular or trapezoidal shape. The passing flow formula over embankment dam crest is like that of

Table 2 Input data to BREACH model

Section width (ft)	Section height (ft)	Average sand diameter (mm)	Shell specific weight $\left(\frac{lb}{ft^3}\right)$	Internal friction angle (degree)	Crest width (ft)
3.2	1	0.5	85	35	0.18
Crest length (ft)	Water elevation at breach initiation (ft)	Crest elevation (ft)	Simulation duration (h)	Input flow (cfs)	Lake area (acres)
3.2	0.8	0.9	0.1	0.08	0.004

Table 3 Input data to HEC-RAS model

Cross-sections number	Cross-sections distance (m)	Breach parameters	Initial and boundary conditions	Simulation duration (min)	Computational time step (s)
60	0.5	Experimental measurements	Experimental conditions	10	1
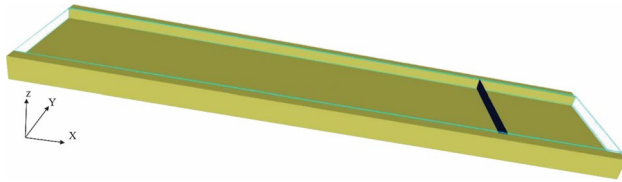
Fig. 3 Experimental channel and open baffle determination at $X = 4$ m in FLOW-3D

the broad-crested weir (Sylvestre J & Sylvestre P, 2018). Equation 3 is used for sediment transport in BREACH model. Table 2 reports the most important data given to the BREACH model according to the experimental setup. The BREACH model generally presents the peak flow and the geometry due to the breach procedure.

2.4 HEC-RAS Numerical Model

In the present article, the HEC-RAS semi-physical model was utilized to estimate the breach flow hydrograph, depth, velocity, and Froude number of the flow at downstream region. Table 3 reveals that the most important data given to the HEC-RAS model according to the experimental setup. The exact explanation of the mentioned model is available in valid sources (Brunner 2016a, b).

2.5 FLOW-3D Numerical Model

The FLOW-3D model belongs to the computational fluid dynamics models. In the present research, the simulation goals include the damping approximation of the flow hydrograph at 4-m distance downstream and the hydraulic parameters estimation due to the physical model breach. To achieve the above-mentioned goals, the measured hydrograph at the weir location was used as the upstream boundary condition. In addition, an open porous plate (a fully open baffle) was defined at $x = 4$ m to obtain the downstream routed hydrograph. Figure 3 displays the mentioned modeling; and Table 4 presents a summary of the input data to the FLOW-3D model. The thorough explanation of the mentioned model is available in valid sources (Flow Science Corporation 2017). The RMSE index can be used to determine the accuracy of numerical models (Eq. 8).

$$\text{RMSE} = \sqrt{\frac{1}{n} \sum_{i=1}^{n} (x_{\text{o}} - x_{\text{p}})^2} \qquad (8)$$

where x_{o} and x_{p} are the observational and predicted data, respectively, and n is data number.

Table 4 Input data to FLOW-3D model

Simulation duration (s)	Turbulence model	Fluid type	Channel dimensions (m)	Channel slope (degree)	Channel roughness (m)
270	RNG	20 °C water	$5 \times 1 \times 0.1$	0.11	0.0005

Mesh size (m)	Boundary condition at $X_{\min}$	Boundary condition at $X_{\max}$	Boundary condition at $Z_{\max}$	Other boundary conditions	Time step at simulation initiation (s)
0.01	Volume flow rate	Outflow	Symmetry	Wall	0.01

Table 5 A comparison of BREACH model outputs and experimental results

Subject	Peak discharge $\left(\frac{l}{s}\right)$	Peak discharge time (s)	Breach section height (cm)	Sediment thickness at breach section (cm)	Downstream maximum water level (cm)
BREACH	28.3	72	29.3	1.2	5.5
Experimental	27.7	125	25	2	6.5

3 Results and Discussion

3.1 BREACH Model Results

Table 5 shows the BREACH model outputs based upon constructed physical model with 30.48-cm height. According to Table 5, the calculated peak flow by the BREACH model is higher than that of the experimental model. Furthermore, its occurrence time has been predicted at a much shorter time. Considering the modeling restrictions in the BREACH model; an appropriate prediction was occurred on the peak discharge. In addition, the predicted maximum water level is 15% less than that of the experimental model. Also, the ratio of breach section height to sediment thickness has been calculated equal to about twice as large as the experimental magnitude.

3.2 HEC-RAS Model Results

3.2.1 Comparison of Reservoir Water Level Variations

Figure 4 reveals the changes in the reservoir water level during the breach process. According to the drawn diagram, at the breach initiation of the experimental model, a slight increase in the water level has occurred. Its reason is related to the relative increase in the reservoir inflow in comparison with the breach outflow. After that a descending trend is observed. Also, the experimental magnitudes are higher than the predicted magnitudes. The RMSE index is computed as 2 for the comparison above.

3.2.2 Comparison of Downstream Water Level Changes

Figure 5 depicts the comparison between the downstream flow levels (at the first section near to physical model). According to Fig. 5; at the initiation of the breach process ($T < 60$ s); the downstream water level was measured as
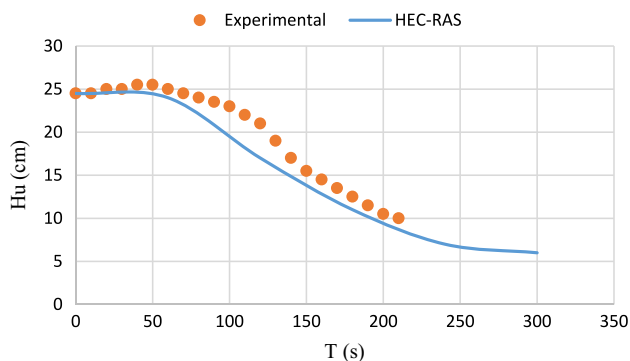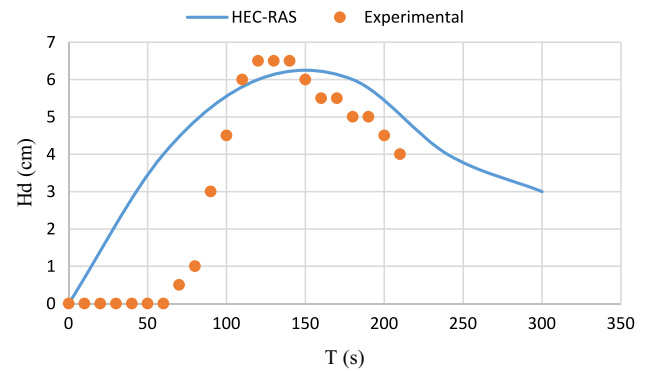

Fig. 5 Downstream flow levels comparison in HEC-RAS

approximately negligible. It confirms that the embankment dams breach process contains a gradual procedure. Moreover, the observed maximum level (6.5 cm) is higher than the predicted maximum level (6 cm). The RMSE index is computed as 1.9 for the comparison above.

3.2.3 Downstream Flow Profile Comparison

Figure 6 demonstrates the comparison between the downstream flow profiles at the peak flow time ($t = 125$ s). Based on Fig. 6; the calculated magnitudes at three points are the same (6 cm), while it begins from 6.5 cm and ends to 4.5 cm in the observed status. The RMSE index is computed as 0.91 for the comparison above.

3.2.4 Changes of Flow Velocity and Froude Number

Figure 7 shows the diagrams of flow velocity and Froude number variations due to breach at downstream section (close to the physical model toe). According to Fig. 7; the maximum flow velocity at downstream section is 0.44 m/s. Also, the maximum Froude number at downstream section was calculated equal to 0.57; indicating that the flow due to the breach process is subcritical flow. The calculation of flow
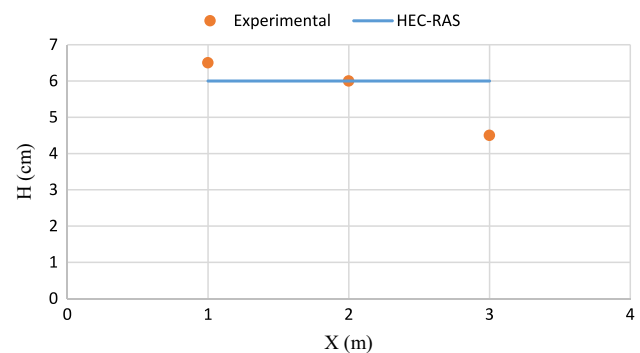

Fig. 4 Variations of lake water level in HEC-RAS

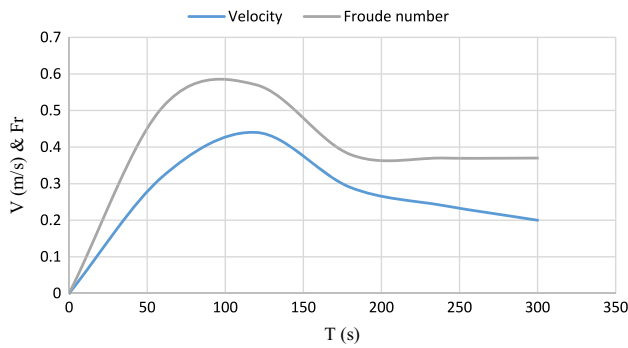

Fig. 6 Downstream flow profile comparison

Fig. 7 Variations of the flow velocity and Froude number at the downstream first section in HEC-RAS
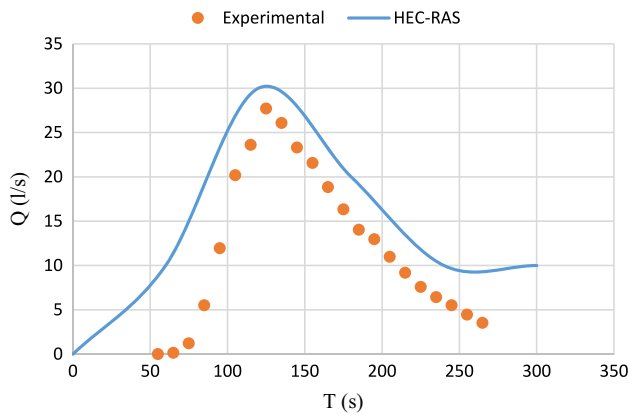
Fig. 8 Comparison of the breach flow hydrographs

velocity by the HEC-RAS model is important; because the flow velocity was not measured at the experimental channel.

3.2.5 Breach Flow Hydrograph Comparison

Figure 8 shows the comparison of breach flow hydrographs. According to Fig. 8; the measured diagram magnitudes are smaller than the calculated diagram magnitudes. The mentioned difference is logical; because the numerical flow hydrograph has been calculated close to the physical model toe. Table 6 compares the HEC-RAS

model outputs and experimental results. The computed peak flow is 30 l/s. Because the flow hydrograph measurement was done at 5.5 m away from the breach section; there is 8% increase in the peak flow calculation. In addition, 5-s reduction at the peak discharge time prediction has occurred. They are in accordance with the flow routing principles. Because there were no experimental thorough tools to measure the discharge and velocity of breach flow; the done calculations by the HEC-RAS model can fill the existing gap.

3.3 FLOW-3D Model Results

To estimate the breach flow hydraulic parameters and to investigate the flow hydrograph damping (at 4 m away from the physical model); the measured flow hydrograph at weir location was given as the upstream boundary condition. The flow depth, velocity, Froude number, and flow hydrograph routing were calculated by the FLOW-3D model.
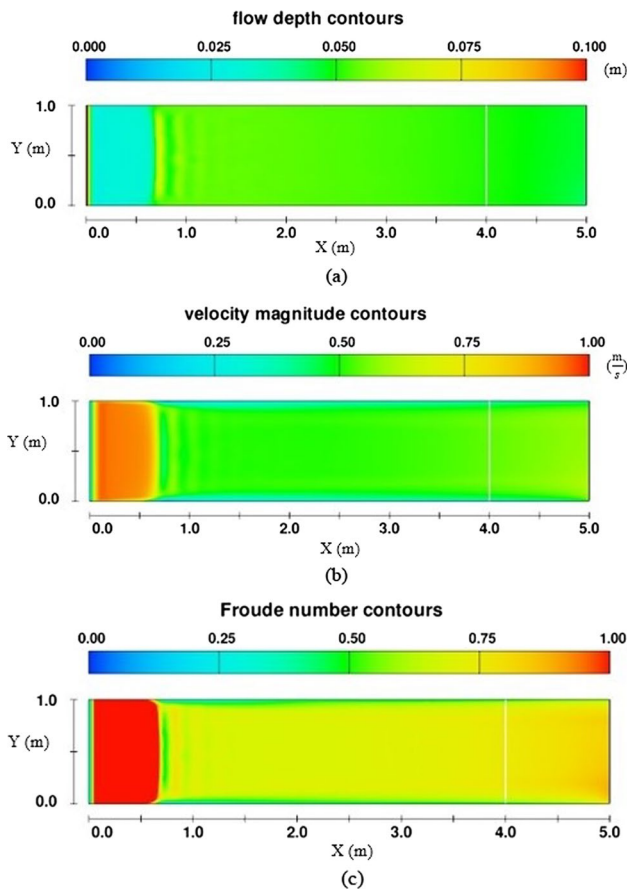
3.3.1 Flow Depth, Velocity, and Froude Number Calculations by the FLOW-3D Model

Figure 9 presents the contours of flow depth, velocity, and Froude number at downstream region at the time which is close to peak discharge occurrence. The predicted magnitudes are in the SI system. As Fig. 9 reveals; at $X \geq 1$ m; the computational maximum depth is 7 cm
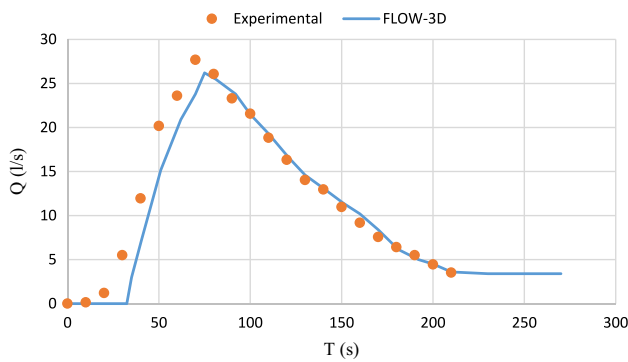
(8% higher than the measured magnitude); maximum velocity is 0.7 m/s; and maximum Froude number is 0.7. The flow velocity prediction is a highly important subject. Since there were no experimental precise tools to measure it. Furthermore, the flow regime is subcritical. Because the Froude number is less than 1.

3.3.2 Investigation of the Flow Hydrograph Routing

Figure 10 depicts the flow hydrograph routing at $X = 4$ m. According to Fig. 10; the upstream peak flow was assumed 27.7 l/s; and its occurrence time was 70 s. At $X = 4$ m, the FLOW-3D model computed the mentioned items 26.2 l/s and 75 s, respectively. The peak flow reduction at 4-m

Table 6 A comparison of HEC-RAS model outputs and experimental results

Subject	Peak discharge $\left(\frac{l}{s}\right)$	Peak discharge time (s)	Maximum velocity $\left(\frac{m}{s}\right)$	Maximum Froude number	Downstream maximum water level (cm)	Lake maximum water level (cm)
HEC-RAS	30	120	0.44	0.57	6	24.5
Experimental	27.7	125			6.5	25.5

Fig. 9 Computational maximum: **a** depth, **b** velocity, and **c** Froude number by FLOW-3D at downstream region at the time which is close to peak discharge occurrence

Fig. 10 Flow hydrograph routing calculation at $X = 4$ m by FLOW-3D

distance downstream was calculated 5%; and its lag time was 5 s. They are in accordance with the flow routing principles. The mentioned method would be implemented to determine the peak flow reduction and its occurrence time at the experimental channels. Table 7 compares the FLOW-3D model outcomes and experimental results.

3.4 Peak Flow Discharge Comparison with the Previous Studies

The experimental results of the peak outflow for the homogeneous earth dam were compared with the empirical relationships of Webby (1996) [Eq. (9)], and Hakimzadeh et al. (2014) [Eq. (10)]. A reasonable agreement was achieved; particularly with the relationship of Hakimzadeh et al. (2014). Table 8 shows the mentioned comparison.

$$Q_p = 0.0443 g^{0.5} V_W^{0.365} H_W^{1.4} \tag{9}$$

$$Q_p = H_W^{2.5} \tag{10}$$

where H_W = height of water before breach; V_W = reservoir storage volume; and g = gravitational acceleration. In the current research, the difference percentages with the empirical relationships of Webby (1996) and Hakimzadeh et al. (2014) are less than 15% and 5%, respectively.

4 Conclusions

This study focuses on software modeling of the overtopping breach phenomenon. Also, the important outputs were compared to the obtained results from the experimental measurements; remarks as below:

The BREACH model exhibits a desired prediction for the peak flow and 15% reduction in calculation of the downstream maximum flow depth. However, it shows a lower accuracy in terms of the peak discharge occurrence time and the breach section height.

According to the HEC-RAS model results, the diagram of reservoir water level variations during the breach process has a descending trend. Whereas it was initially observed an ascending trend; and then, it experienced a downward trend in the observed status. Also, the

Table 7 A comparison of the FLOW-3D model outcomes and the experimental results

Subject	Downstream peak discharge $\left(\frac{l}{s}\right)$	Peak discharge time (s)	Maximum velocity $\left(\frac{m}{s}\right)$	Maximum Froude number	Downstream max water level (cm)
FLOW-3D	26.2	75	0.7	0.7	7
Experimental	27.7	70			6.5

Table 8 A comparison of peak discharge $\left(\frac{l}{s}\right)$ with the empirical relationships

Subject	Current study	Webby (1996)	Hakimzadeh et al. (2014)
$H = 1$ ft (BREACH)	28.3	33	29.7
$H = 27$ cm (HEC-RAS)	30	33	29.7

mentioned model presented a suitable prediction in terms of the peak discharge (higher than that calculated by the BREACH model), its occurrence time (5-s difference with observed status), and downstream flow depth. In addition, the calculated flow hydrograph was according to the flow routing principles. Moreover, the downstream flow regime was determined to be subcritical flow for the constructed model.

The FLOW-3D model calculated the peak discharge damping equal to 5% at 4-m distance downstream. Additionally, there was 5-s difference in the peak discharge occurrence time in comparison with the upstream hydrograph. Besides, the flow depth, velocity, and Froude number were calculated by the mentioned model.

The above-mentioned results may create a comprehensive vision on the hydraulic results of physical models for the overtopping breach.

Author Contributions All authors contributed to the concept and the development of the idea. Mahdi Ebrahimi and Sayed Mohammad Hadi Meshkati contributed to the experimental setup and generation of results. Mahdi Ebrahimi and Mirali Mohammadi contributed to the revision of the manuscript. All authors read and approved the final manuscript.

Data Availability All relevant data are included in the paper or its supplementary information.

Declarations

Conflict of Interest The authors have no competing interests to declare that are relevant to the content of this article.**.**

References

Association of state dam safety officials (2023) Kentucky, USA. Available from https://damsafety.org

ASTM D1557 (2007) Standard test methods for laboratory compaction characteristics of soil using standard effort. West Conshohocken, PA, USA

ASTM D422–63 (2002) Standard test method for particle size analysis of soils

Azimi H, Shabanlou S (2016) Comparison of subcritical and supercritical flow patterns within triangular channels along the side weir. Int J Nonlinear Sci Numer Simul 17(7–8):361–368

Azimi H, Shabanlou S (2018) Numerical study of bed slope change effect of circular channel with side weir in supercritical flow conditions. Appl Water Sci 8(6):166

Azimi H, Shabanlou S, Kardar S (2017) Characteristics of hydraulic jump in U-shaped channels. Arab J Sci Eng 42:3751–3760

Brunner GW (2016) HEC-RAS Reference Manual, version 5.0. Hydrologic Engineering Center, Institute for Water Resources, US Army Corps of Engineers, Davis, California

Brunner GW (2016) HEC-RAS user's Manual, version 5.0. Hydrologic Engineering Center, Institute for Water Resources, US Army Corps of Engineers, Davis, California

Chanson H, Wang H (2013) Unsteady discharge calibration of a large V-notch weir. Flow Meas Instrum 29:19–24

Committee on Dam Safety (2019) ICOLD incident database bulletin 99 update: statistical analysis of dam failures, technical report, international commission on large dams. Available from: https://www.icoldchile.cl/boletines/188.pdf

Engomoen B, Witter DT, Knight K, Luebke TA (2014) Design Standards No 13: Embankment Dams. United States Bureau of Reclamation

Flow Science Corporation (2017) Flow-3D v11.0 User Manual. Available from: http://flow3d.com

Froehlich DC (2016) Predicting peak discharge from gradually breached embankment dam. J Hydrol Eng 21(11):04016041

Hakimzadeh H, Nourani V, Amini AB (2014) Genetic programming simulation of dam breach hydrograph and peak outflow discharge. J Hydrol Eng 19:757–768

Hooshyaripor F, Tahershamsi A, Golian S (2014) Application of copula method and neural networks for predicting peak outflow from breached embankments. J Hydro-Environ Res 8(3):292–303

Irmakunal CI (2019) Two-dimensional dam break analyses of Berdan dam. MSC thesis, Middle East Technical University, Turkey

kumar Gupta A, Narang I, Goyal P, (2020) Dam break analysis of JAWAI dam PALI, Rajasthan using HEC-RAS. IOSR J Mech Civ Eng 17(2):43–52

Mo C, Cen W, Le X, Ban H, Ruan Y, Lai S, Shen Y (2023) Simulation of dam-break flood and risk assessment: a case study of Chengbi river dam in Baise, China. J Hydroinformatics 25(4):1276–1294

Morris M, Kortenhaus A, Visser P (2009) Modelling breach initiation and growth. FLOODsite report: T06–08–02, FLOODsite Consortium, Wallingford, UK

Novak P, Moffat AIB, Nalluri C, Narayanan RAIB (2017) Hydraulic structures. CRC Press

Pierce MW, Thornton CI, Abt SR (2010) Predicting peak outflow from breached embankment dams. J Hydrol Eng 15(5):338–349

Saberi O (2016) Embankment dam failure outflow hydrograph development. PhD thesis, Graz University of Technology, Austria

Sylvestre J, Sylvestre P (2018) User's guide for BRCH GUI. 2018. Available from: http://rivermechanics.net

USACE) 2004) General design and construction considerations for Earth and rockfill dams, US Army Corps of Engineers, Washington DC, USA

USBR (1987) Design of small dams, Bureau of Reclamation, Water Resources Technical Publication

Versteeg HK, Malalasekera W (2007) An introduction to computational fluid dynamics: the finite volume method. Pearson education

Wang Z, Bowles DS (2006) Three-dimensional non-cohesive earthen dam breach model. Part 1: theory and methodology. Adv Water Resour 29(10):1528–1545

Webby MG (1996) Discussion of peak outflow from breached embankment dam by David C. Froehlich. J Water Resour Plan Manag 122(4):316–317

Wu W, Marsooli R, He Z (2012) Depth-averaged two-dimensional model of unsteady flow and sediment transport due to noncohesive embankment break/breaching. J Hydraul Eng 138(6):503–516

Xu Y, Zhang LM (2009) Breaching parameters for earth and rockfill dams. J Geotech Geoenviron Eng 135(12):1957–1970